High T_c superconductor voltage–current simulator and the pulse method of measuring critical current*

L.F. Goodrich

Center for Electronics and Electrical Engineering, National Institute of Standards and Technology, Boulder, CO 80303, USA

Received 6 September 1990; revised 8 May 1991

A passive voltage – current ($V-I$) simulator has been developed and tested using conventional direct current (d.c.) and pulse current methods. The simulator was designed to generate the extremely non-linear $V-I$ characteristic of a superconductor and has a similar power-law behaviour. It is intended to be used to test various components of the measurement system such as instrumentation, measurement method and data analysis software, to determine the transport critical current, I_c, or critical current density, J_c, of a superconductor. This simulator does not emulate all the subtle effects of flux flow in a superconductor. However, it approximates a superconductor's major static and dynamic electrical characteristics. The simulator is therefore a necessary but incomplete test of a measurement system. Critical currents obtained on the simulator using the pulse and d.c. methods are compared and show close agreement. Also, preliminary comparisons of methods using bulk and thin film YBCO samples are given.

Keywords: high T_c superconductors; critical currents; measuring methods

A general introduction to the measurement of critical current for conventional and high T_c superconductors can be found elsewhere[1,2]. It suffices here to say that the transport I_c is an important parameter for characterizing a superconductor; it is a measure of the conductor's current carrying capacity.

All functional I_c definitions are based on an I_c criterion and the measurement of a non-zero voltage. The superconductor's voltage–current ($V-I$) characteristic can usually be approximated by the empirical power-law equation

$$V = V_0(I/I_0)^n \quad (1)$$

where I_0 is a reference current at a voltage V_0 and n reflects the general shape of the $V-I$ curve. Typical values of n range from 10 to 100. Specifically, n indicates the abruptness of the transition from the superconducting to the normal state. The voltage characteristic that is modelled by Equation (1) is caused by the steady state flow of magnetic flux in the specimen[1]. Unlike thermal runaway or flux jump, this is a stable and reversible condition.

The two most commonly used I_c criteria are the electric field criterion, E_c, and the resistivity criterion, ρ_c. Both criteria are based on the measurement of a finite voltage, V_c, across the test specimen. It is often difficult to obtain a criterion that is low enough to be relevant for superconductor applications.

I_c measurement methods

D.c. method

In the d.c. transport method, a direct current is injected into the superconductor while the voltage across it is measured. The superconductor's $V-I$ characteristic is determined by recording the voltage as the current is increased. The critical current is determined by applying a criterion to the measured $V-I$ curve. An example of a superconductor simulator's $V-I$ curve is given in *Figure 1*. The d.c. measurement technique is preferred because it is conceptually simple and it closely approximates a superconductor's actual use.

There are two variations on the d.c. method. One variation is to sweep the current at a steady rate with time (continuous d.c. method) and record the voltage and current. The current is inferred from the measured voltage drop across a four-wire standard resistor. The other variation is to ramp the current to various predetermined current set points and hold the current constant (stepped d.c. method) while the voltage and current are measured and averaged. This method requires a computer to determine the set points, ramp

0011 – 2275/91/080720 – 08

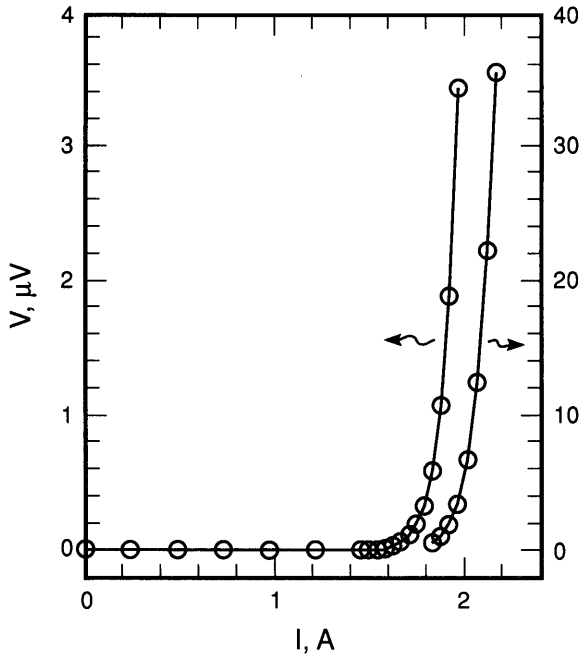

Figure 1 Plot of voltage *versus* current for superconductor simulator 2 taken using the stepped d.c. method

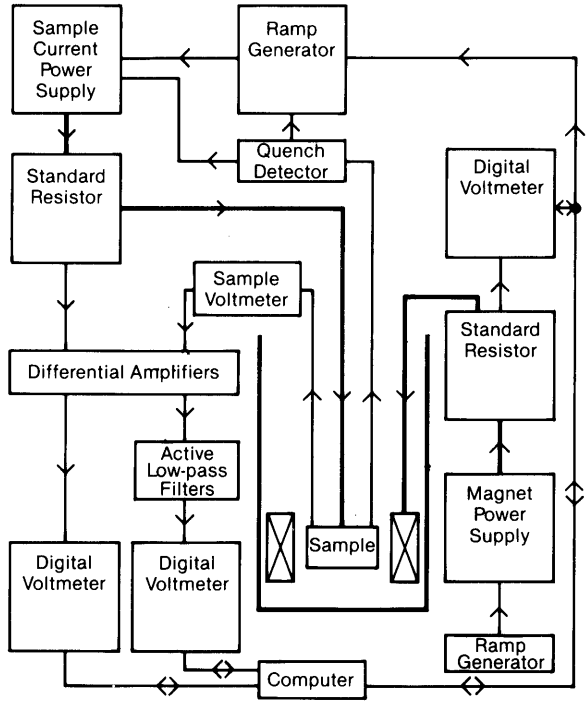

Figure 2 Block diagram of critical current measurement system using the d.c. method

the current and acquire the data. In either variation, the current is virtually at steady state. The typical ramp time from zero to I_c is 100 s for the continuous method. In the stepped d.c. method, the current is ramped between set points in a few tenths of a second and held constant for a few seconds at each set point. The basic difference between these two d.c. methods is that the stepped method determines a number of points along the $V-I$ curve more precisely, while the continuous method more completely determines the $V-I$ curve. The stepped method reduces the effect of inductive voltage. It also allows time for sample motion due to the changing Lorentz force and its associated voltage to decay. Typically, there is less than 0.2% difference between the values of I_c determined by these two d.c. methods. This precision is limited by the accuracy of the continuous method and the limitations of fitting small regions of the $V-I$ curve to Equation (1).

A block diagram of a d.c. critical current measurement system is given in *Figure 2*. The sample voltmeter is a d.c. analogue nanovoltmeter with an amplified analogue output. The output signal is fed through a differential amplifier and an active low-pass filter to a digital voltmeter which can communicate with a computer. The sample current is supplied by a battery powered current supply[3]. If the voltage readings are averaged over a time of 1–2 s, the active filter is not necessary.

All of the d.c. data presented here were acquired using the stepped method. The first and the last points of each curve (total of 22–25 points) were acquired with zero sample current to allow for the determination of offset and thermoelectric voltages. Four parameters were used to calculate the non-zero current set points: the full scale voltage of the voltmeter, the current that corresponds to this voltage, the approximate n value of the $V-I$ curve and the voltage noise level. The current set points are calculated based on two different premises: approximately equally spaced currents on a linear scale for the lower currents and approximately equally spaced voltages on a logarithmic scale. The current set point that separates these two regions is the current at which the sample voltage should (ideally) be just below the voltage noise level. The points on *Figure 1* were determined using this algorithm.

Pulse method

In the pulse current method, the current starts at zero, is ramped quickly to a relatively constant level, the voltage drop along the conductor is measured and the current is ramped to zero again. In order to allow for any voltage offset corrections, the sample voltage is also measured in the two zero current regions. A series of such pulses together determine the general shape of the $V-I$ characteristic using a similar algorithm as described in the stepped d.c. method. The duration of each pulse is typically 1–10 ms. This determines the bandwidth necessary for the voltage sensing device. A significant voltage can be induced by the time derivative of the current since the current is changed within a time duration on the order of 0.1 ms. Thus, it is important to verify that the measurement system is relatively insensitive to inductive voltage spikes.

A block diagram for a pulse current critical current measurement system is given in *Figure 3*. The sample voltage measurement device is a differential amplifier with its output fed to a digital processing oscilloscope. Simultaneous readings of control voltage, current and sample voltage were acquired every 100 μs and appropriate averages were calculated. For the pulse data presented here (except for the 5 s pulses), the bandpass of the differential amplifiers was 0–10 kHz for the control voltage and sample current, and 0–3 kHz for the

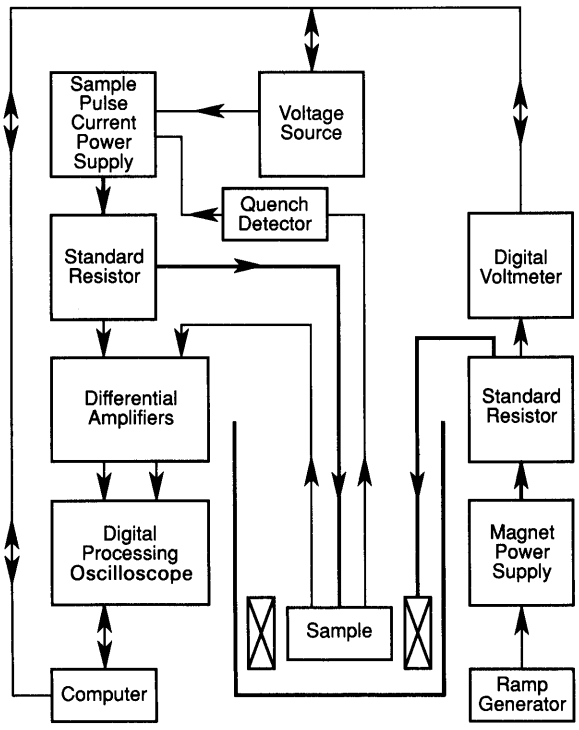

Figure 3 Block diagram of critical current measurement system using the pulse method

sample voltage. The sample current is supplied by a modified battery powered current supply.

The pulse method is used to determine the critical current because it reduces the contact heating by reducing the duty cycle of the current[4,5]. Methods of making low resistance contacts exist[6]; however, small samples and extra processing may limit their implementation. There are a number of measurement issues concerning the pulse method. These include the dynamics of magnetic flux motion, voltage sensitivity, inductive voltages and continuous or stick-slip sample motion. These effects make it more difficult to determine the correct critical current and may, in fact, limit the accuracy of pulse measurements.

Passive simulator

In previous publications[7,8], passive (single components and no internal power source) and active (using operational amplifiers) $V-I$ simulators were described with an emphasis on the active device. The active device has some advantages since it is readily adjustable and can be used in high current systems. The advantage of the passive device is its simplicity in construction, use and response. The $V-I$ characteristic of this passive simulator is not expected to depend on the measurement method based on fundamental electronic circuit analysis for reasonable frequencies. The passive simulator is well suited for a simple comparison of different measurement methods and interlaboratory comparisons of measurements. The simulator is substituted for the sample and all measurements are taken at room temperature. The simulator has a low temperature dependence ($\approx 0.3\%\ °C^{-1}$) and is expected to have only a small variation with time and use. In interlaboratory comparisons, the simulators could be measured by a central laboratory before and after interlaboratory testing to check for possible changes.

A circuit diagram for the passive simulator is given in *Figure 4*. There is a main current branch consisting of no. 14 AWG (or larger) copper wire and no. 19 AWG resistance wire. The voltage drop along part of the resistance wire, load resistance R1, drives a smaller current in a parallel branch. This branch has a current-limiting resistor, R2, the sample resistance, R3, and a diode or Zener diode (forward biased). This diode causes a non-linear current to flow in the parallel branch compared to the current flow in the main branch. Thus the voltage drop across R3 in non-linear with respect to the main current. Three voltage taps are shown on R3: a pair consisting of common and low inductance, L, and another pair consisting of common and high L. Low and high L refers to the relative magnitude of the mutual inductance between the main current and the area enclosed by the voltage tap pair and R3. It is important to route the wires such that the inductive voltage is positive (same polarity as the sample voltage) to test the measurement technique. In the actual device, these two pairs of voltage taps are attached to a number of connectors to facilitate measurements with various devices. The value of R3 should be kept small in order to more closely simulate the impedance of a superconductor. The voltage taps on R2 provide a signal that is larger than the sample voltage by a fixed factor. This can be used to check the precision and accuracy of the sample voltage. The construction was designed to reduce thermoelectric voltages (the load resistor is outside the box and away from the other components) and to have a low self-inductance (the wires are routed in a bifilar manner). It is important to have a low self-inductance in the wiring and resistors so that the response will be relatively independent of measurement method.

To a limited extent, the circuit components can be selected to vary I_c and n. The simulator requires a load voltage of ≈ 0.7 V, so power dissipation becomes a limiting factor. The value of R1 determines the approximate value of I_c. The selection of the diode can vary n from ≈ 10 to 25. The relative values of the resistors in combination with the diode characteristic determine the overall shape of the $V-I$ curve of the simulator.

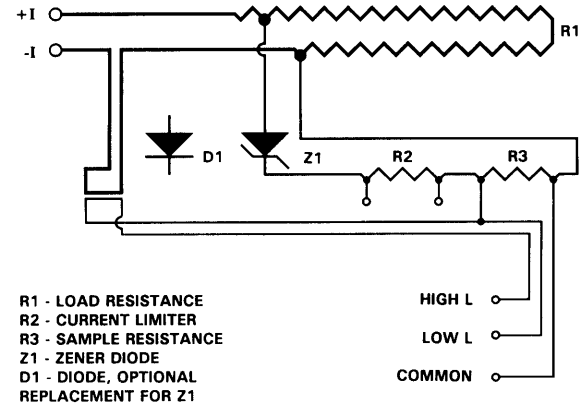

Figure 4 Circuit diagram of the passive simulator. The main current was limited by a 3 A fuse

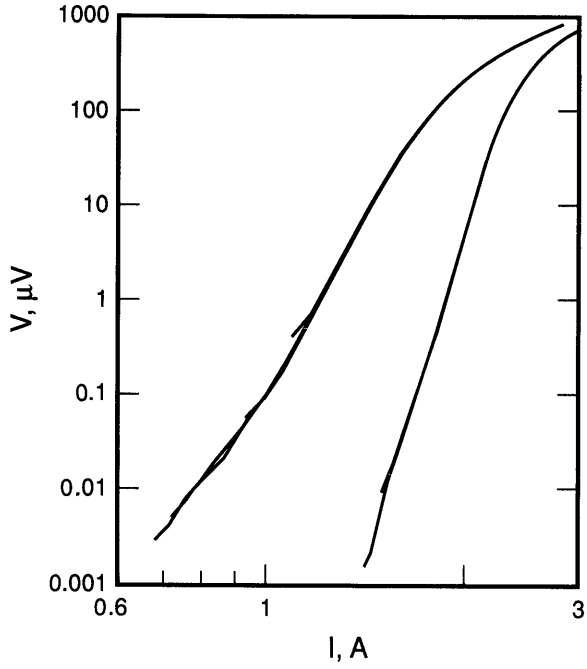

Figure 5 Fully logarithmic plot of voltage *versus* current data for two simulators. Simulator 1 (left curve) R1 = 0.38 Ω, R2 = 10 Ω, R3 = 0.034 Ω, D1 = 1N-4004. Simulator 2 (right curve): R1 = 0.35 Ω, R2 = 8 Ω, R3 = 0.034 Ω, Z1 = 1N-5252B

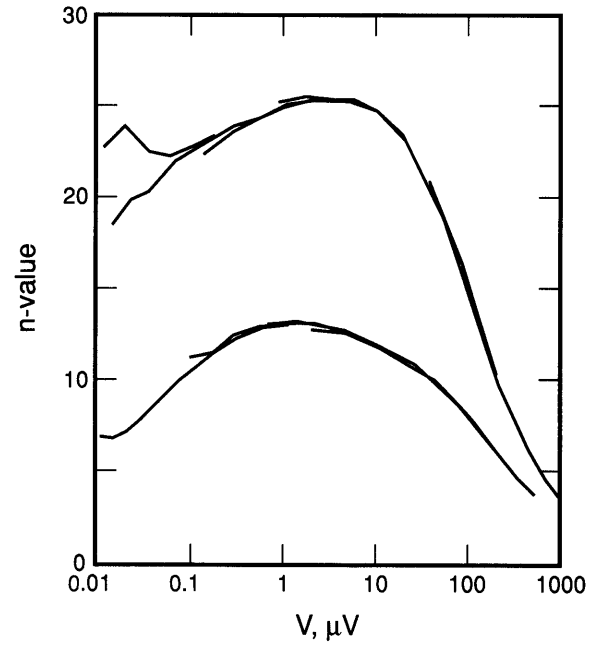

Figure 6 Plot of the *n* value *versus* logarithmic voltage for simulators 1 (lower curve) and 2 (upper curve)

Two simulators have been constructed and tested. A full logarithmic plot of voltage *versus* current for both simulators is given in *Figure 5*. A wide range of voltage data, 1 nV to 1 mV, were acquired on four voltmeter ranges, and some of the starting points of each range can be seen in *Figure 5*. For each simulator, the voltage at currents below these plotted curves was zero within the precision of the measurement. Normally, this plot would be based on electric field or resistivity, but these criteria are somewhat artificial for the simulator. The main difference between these two simulators was the choice of the diode: simulator 1 had a rectifying diode (1N-4004) that gave a maximum n of ≈ 13 and simulator 2 had a forward-biased 24-V Zener diode (1N 5252B) that gave a maximum n of ≈ 25.

A plot of n value *versus* voltage for both simulators is given in *Figure 6*. The n values were determined using sets consisting of three pairs of $V-I$ points. Because of the set-point algorithm, the voltage of the third point was typically a factor of three greater than the voltage of the first point in each set. The n value was assigned to the middle voltage point. If power dissipation is low, the decreased n value at higher voltages is similar to that observed for superconductors. This is largely determined by the current-limiting resistor, R2. The variation in n observed below 0.1 μV is due to the non-zero noise level and the attendant difficulty of accurate determination of n. The resistors were chosen so that the peak in the curve of n *versus* voltage is in the region of 1−10 μV. The higher voltages are presented in *Figure 6* for completeness. The $V-I$ characteristics of the current-limiting resistor, R2, would have significantly higher n values at the higher voltages.

The actual shape of the simulator $V-I$ curves in the region near 1 mV is linear with a non-zero current intercept. Because of the current intercept, fitting this region to Equation (1) will give an apparent n of 3−5 instead of 1. For voltages below 30 and 100 μV for simulators 1 and 2, respectively, the linearity of the fully logarithmic plot in *Figure 5* indicates that Equation (1) is a good approximation of the curve.

Comparisons of methods using simulators

Figure 7 is a fully logarithmic plot of the $V-I$ characteristic of simulator 2 using the two methods. Two curves were acquired using the d.c. method (stepped) and are shown as solid lines for clarity. These two curves are almost identical except for the region near 0.1 μV. Two symbol types are used to show the individual data points of two curves determined by the pulse method. The triangle is used for the 5 ms pulse-duration data and the circle for 10 ms pulse-width data. The 10 ms pulse-duration data have better precision; however, the uncertainty in the voltage is still ≈ 0.3 μV. In contrast, the uncertainty of the d.c. method is ≈ 10 nV. For the simulators, the difference between the d.c. and pulse methods for determining the critical current at 10 μV was $\approx 0.2\%$.

Figure 8 is an enlargement of the curves shown on *Figure 7* with the addition of two 5 s single pulses. One hundred individual $V-I$ points make up each of the two jagged line segments. For these long pulse durations, the bandpass of the differential amplifier was decreased to 0 to 30 Hz and a reading was recorded every 50 ms. This type of data was taken to study any time dependence of the pulse measurement system. These line segments are consistent with the 5 and 10 ms pulse width data points, thus indicating a lack of time dependence. The slight ($\approx 1\%$) drift in the current during each 5 s pulse gave these pulses a non-zero length on the plot.

Although these curves were acquired using the high L voltage taps, they are representative of the data taken on

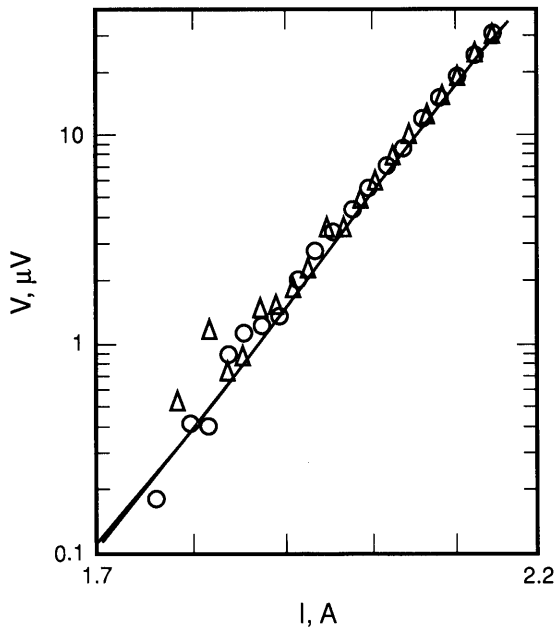

Figure 7 Fully logarithmic plot of voltage *versus* current data obtained on simulator 2 using the d.c. method (solid lines) and the pulse method (Δ , 5 ms pulse; O , 10 ms pulse)

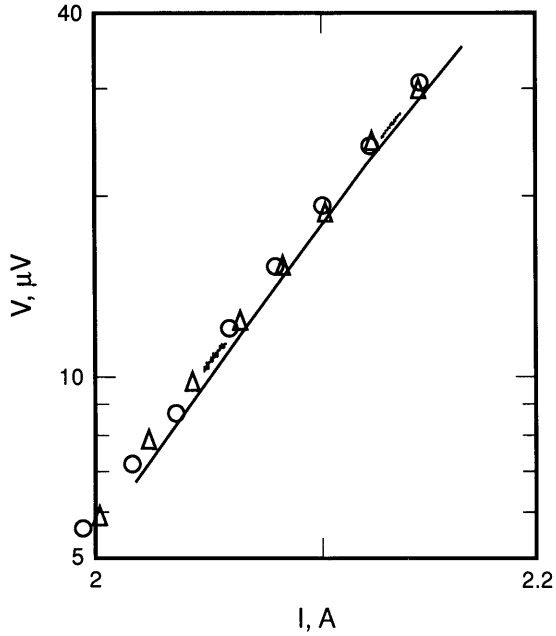

Figure 8 Enlargement of *Figure 7* with the addition of individual *V–I* points from two 5 s pulses (jagged line segments)

both simulators using either pair of voltage taps (low or high *L*). The inductance was not quantified, but the inductive voltage spike was ≈30 μV. This turned out to be about four times what was achieved on the superconductive sample with a similar current pulse. It is important to verify that the equipment and software are insensitive to inductive voltage spikes.

The pulse data were dependent on the grounding and shielding conditions. This was most evident for the current pulses that were well below the I_c, where the voltage should have been zero. The voltage shifted slightly positive or negative during the current pulse relative to the voltage measured during the zero current regions on either side of the current pulse. These offsets were fairly constant for the lower currents and seemed to bias the measured voltage all along the *V–I* curve. Modifying the ground conditions resulted in pulse data that were either slightly above or below the d.c. data for positive or negative voltage shifts, respectively. In all cases, the curves for the two methods approached each other as the voltage was increased. These slight voltage shifts are thought to be caused by ground loops or common-mode voltages. Results with longer pulse durations indicated that these shifts had no time dependence. No correction for this effect was made in the data presented in this paper. In all cases, the magnitude of this effect was less than 0.5 μV. If a correction were made, the d.c. and pulse curves would be in better agreement. Similar observations were made for the pulse data on superconducting samples.

Comparisons of methods using superconductors

A laser-ablated YBCO thin film was measured using both the d.c. and the pulse measurement methods. To quantify any changes in the film characteristics, *V–I* curves were acquired using the d.c. method before and after each set of pulse curves. The sample was measured while immersed in liquid nitrogen (76 K) and held in a water-cooled copper wire and iron pole piece magnet. The applied magnetic field was perpendicular to the sample current in the plane of the film and perpendicular to the c-axis of the film. The film was patterned with a width of 500 μm and the voltage taps were separated by 5 mm. The thickness of the film was ≈0.3 μm, so the cross-sectional area was $\approx 1.5 \times 10^{-6}$ cm^2. The critical current density was $\approx 1.0 \times 10^6$ A cm^{-2} at zero field, 8.7×10^5 A cm^{-2} at 0.1 T and 3.2×10^5 A cm^{-2} at 1 T, using a 1 μV cm^{-1} criterion. The current and voltage pads were coated with silver to reduce the contact resistance. The voltage and current connections to the sample were made using Be–Cu springs coated with In–Ag solder. The sum of the resistances of both current contacts was ≈8 mΩ and was independent of current and measurement method (d.c. or pulse). The total power dissipation at 1.8 A was ≈26 mW.

An example of the pulse waveforms *versus* time is given in *Figure 9*. The pulse width is 5 ms and is centred on the plot between two zero current regions. The upper pulse is the control voltage signal that is fed to the pulse-current supply. The middle waveform is the sample current and closely tracks the control voltage. Both the control voltage and the sample current are slightly rounded at the beginning of the pulse. The rise time of the current is a few tenths of a millisecond, but this rounding occurs over a time of ≈1 ms. The drift in the current over the last 3.5 ms of the pulse is less than 0.2%. The bottom waveform is the sample voltage with an offset of ≈28 μV during the pulse. It has positive and negative inductive spikes at the beginning and end of the pulse, respectively. These spikes are almost coincident with the maximum change in current with time. The positive spike is followed by a decrease in sample voltage, then an increase in voltage. This occurs because

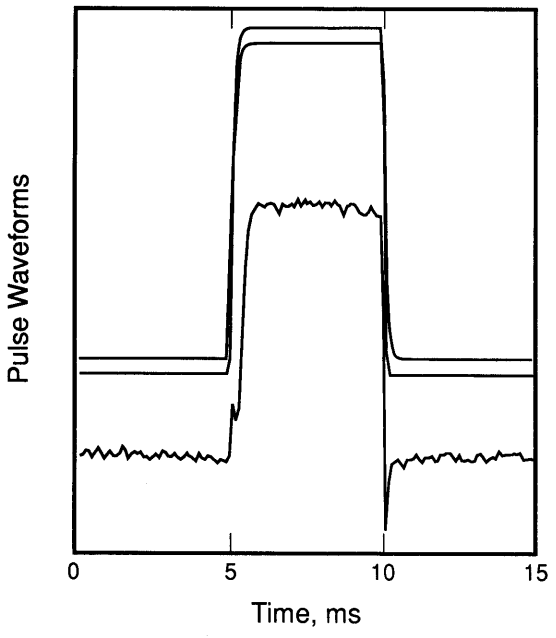

Figure 9 Plot of current supply control voltage (top curve), sample current (middle curve) and sample voltage (bottom curve) as a function of time for a single current pulse

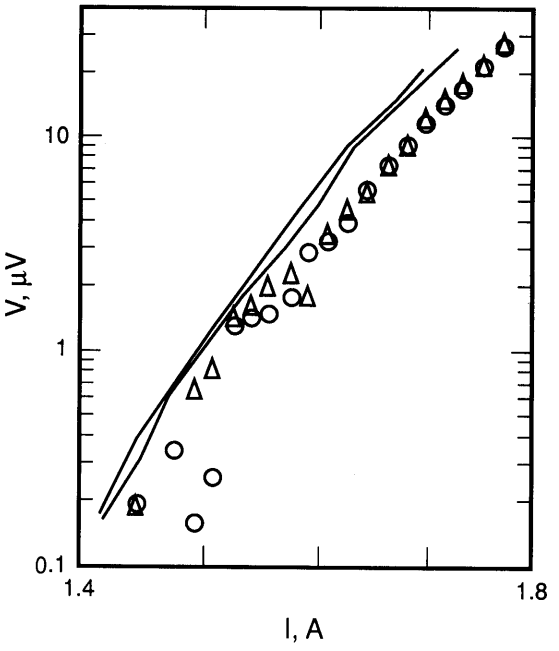

Figure 10 Fully logarithmic plot of voltage *versus* current data obtained on a thin film sample at 76 K with zero magnetic field using the d.c. method (solid lines, uppermost curve after pulse data) and the pulse method (Δ and O , 5 ms pulses)

the rounded current waveform is exaggerated by the $V-I$ relationship in Equation (1), thus resulting in a voltage drop that is lower than the inductive spike for the early part of the current pulse. The individual pairs of voltage and current points during a single pulse (including these initial points) are consistent with the pulse-determined $V-I$ curve to within experimental uncertainties. Observations made on the low and high L voltage taps of the simulators confirm this effect. The computer data analysis software was designed to avoid the transient regions of the waveforms.

A fully logarithmic plot of voltage *versus* current with zero applied magnetic field at 76 K for the two methods is shown in *Figure 10*. Two curves were acquired using the d.c. method (stepped) and are shown as solid lines for clarity. The uppermost curve was taken after the pulse data and the lower d.c. curve was taken before the pulse data. These two curves show a slight shift in the $V-I$ characteristic of the film. Two symbol types were used to show the individual data points of two pulse method curves. Both of these curves used 5 ms pulses. The uncertainty in the pulse voltages was ≈ 0.5 μV for these measurements. However, the pulse and d.c. curves do not approach each other as the voltage is increased. At 10 μV (20 μV cm^{-1}) the difference in the I_c values determined by the two methods was $\approx 3\%$, with the higher I_c obtained with the pulse method.

Figure 11 is an enlargement of the curves shown in *Figure 10* with the addition of a single 5 s pulse. One hundred individual voltage and current readings make up the dotted line starting near the centre of the plot. These data show a time dependence of the pulse measurement. There was a slight ($\approx 1\%$) drift in the current during the 5 s pulse. The dotted line segment starts near the other pulse data and ends just above an extension of the d.c. curves. The amount by which the top end of this dotted line segment is above the d.c. curves may be within the variability of the film characteristic and the relative calibrations of the two measurement systems. The time for the voltage to traverse the first half of the dotted line segment was ≈ 0.7 s. This time may be the approximate time constant of this effect.

Comparisons of pulse and d.c. data were made at 0.1 and 1.0 T. The 0.1 T data were very similar to the zero field data. The I_c was slightly lower at 0.1 T. The pulse method gave a value of I_c that was 2.5% higher than

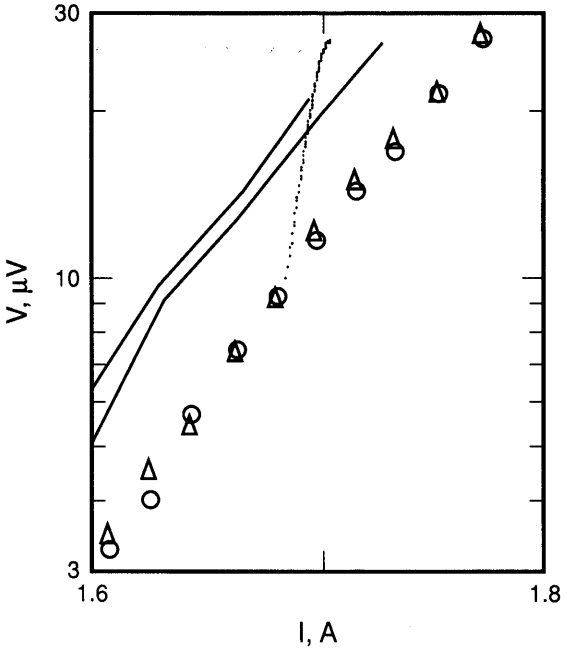

Figure 11 Enlargement of *Figure 10* with the addition of individual $V-I$ points from a 5 s pulse

that of the d.c. method. At 1 T, the d.c. and pulse curves were very close; the pulse method gave a value of I_c that was only 1% higher than that of the d.c. method. There was also a smaller difference between the two d.c. curves that were acquired before and after the pulse data at 1 T. With this higher precision, it was possible to see that a 5 s long pulse also started on the pulse curves and ended near the d.c. curves even though the curves were close together.

Sample motion was a significant problem with the pulse measurement at non-zero fields, since current pulses create Lorentz force pulses on the sample. This sample motion can induce an interfering voltage on the voltage taps. An effort was made to reduce the area formed by the voltages taps and the length of sample between them. Also, adjustments in mechanical restraint were made to decrease the amplitude of the sample motion relative to the magnet. Even with these changes, the noise at 1 T was two to three times the noise at zero field.

The degradation with time and mounting method was investigated on the thin film specimen whose data are presented here. The specimen was mounted with pressure contacts, measured, dismounted and stored in a desiccator three times over the course of three months. The degradation of I_c was $\approx 6\%$ over this time period. The specimen was then mounted using In–3%Ag solder contacts. The degradation in I_c was $\approx 4\%$, compared to data taken with pressure contacts three days earlier.

The solder contacts were made so that the comparison of d.c. and pulse methods could be made with lower contact resistance and, therefore, less contact heating. No solder flux was used when soldering the presoldered copper foils to the silver pads, and a minimum time and temperature was used to reduce possible degradation. The total resistance of the two current contacts was ≈ 0.5 mΩ, which would dissipate ≈ 1.4 mW of power compared to 26 mW for the other data presented here. The comparison of d.c. and pulse methods on the specimen with soldered contacts is showed on *Figure 12*. There are four d.c. curves, two 5 ms pulse curves and three 5 s pulses (jagged line segments) on this figure. The agreement was good, within 1% for a sample voltage from 1 to 70 μV. The 5 s pulses were consistent with the $V-I$ characteristics determined using 5 and 10 ms pulses. Data with 0.1 and 1 T applied fields also had virtually identical characteristics for the two methods. The agreement of the two methods was similar to that observed on the simulator (*Figures 7* and *8*). These data suggest that contact heating was the source of any difference between the two measurement methods presented here.

The heat flux (power dissipated per unit surface area) for these two types of current contacts is difficult to quantify. The surface area of each current contact was ≈ 9 mm^2 and the silver was ≈ 0.5 μm thick. The surface of the patterned film was horizontal in the liquid nitrogen bath. Each pressure contact had an approximate area of 0.1 mm^2, which would result in a heat flux of ≈ 13 W cm^{-2} in the worst case. This heat flux is close to the transition from nucleate to film boiling (15 W cm^{-2}). The heat flux will be significantly lower than 13 W cm^{-2}, since the current will spread in the silver and the heat will flow through the silver and BeCu to surrounding areas, then into the liquid nitrogen. The

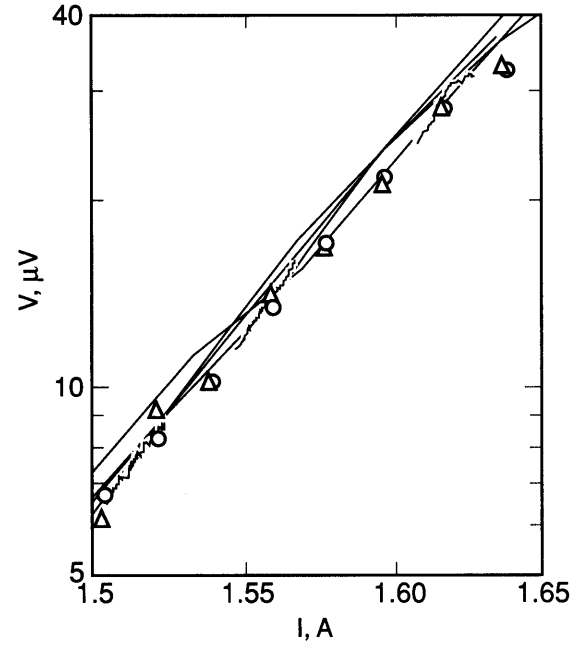

Figure 12 Fully logarithmic plot of voltage *versus* current data obtained on a thin film sample with low resistance contacts at 76 K with zero magnetic field using the d.c. method (solid lines), the pulse method (Δ and O , 5 ms pulses) and individual $V-I$ points from three 5 s pulses (jagged line segments)

effective area of the pressure contact can be estimated using the area and resistance of the solder contact and the resistance of the pressure contact, assuming the silver–YBCO interface resistance is uniform. This gives an effective area of ≈ 0.44 mm^2 and a heat flux of ≈ 3 W cm^{-2}. There still can be a noticeable rise in the specimen temperature. Each solder current contact had an area of ≈ 7 mm^2, which would result in a heat flux of ≈ 0.01 W cm^{-2}. With this heat flux, the specimen temperature will be very close to the bath temperature.

A bulk sintered YBCO sample was measured using both the d.c. and the pulse measurement methods. The lower current density of the bulk sample (≈ 50 A cm^{-2} at zero field) allowed comparison of the two methods over a wide range of I_c criteria. The difference in I_c did not depend on the criterion. The data on the bulk sample showed a larger shift of the $V-I$ characteristic with subsequent measurements compared to data on the thin film sample. These shifts were approximately reversed by thermal cycling the specimen above its transition temperature. This suggests that subsequent measurement changes the flux distribution within the sample. These shifts limited the comparison of measurement methods. However, nested measurements indicated a trend of less than 2% difference in I_c between the two methods for criteria between 10 and 50 μV cm^{-1}.

Discussion

The measurement of I_c is more complicated than commonly perceived and is sensitive to a variety of subtle variables. Small changes in these measurement variables can result in large changes in the measured I_c. This is evidenced by the results of two recent high T_c

interlaboratory comparisons (Japan, January 1988[9]; DARPA, April 1989[10]) where variation in measured I_c was as large as ±50%. There are many possible sources of measurement variability including sample inhomogeneity, sample damage and contact resistance, in addition to the type of measurement system and technique. A passive simulator is the first step in the process to determine the major sources of measurement variability.

There are a number of possible uses for a superconductor simulator ranging from a simple non-linear $V-I$ curve generator to a standard reference device. The design and construction of a non-linear $V-I$ curve generator is not critical. However, for a standard reference device used to test a critical current measurement system, the construction, and in particular the routing of the wires, is important in order to approximate the major static and dynamic electrical characteristics of a superconductor. A superconducting sample has very little power dissipation, small thermoelectric voltages (if immersed in a bath), low self-inductance and a finite mutual inductance with the voltage taps. The wires in the simulator need to be routed to reduce unwanted effects of power dissipation and high self-inductance, while maintaining the effects of mutual inductance between the main sample current and the voltage taps.

The choice of simulator components may affect the overall stability of the $V-I$ characteristic with temperature, time and use. Copies of this circuit may have slightly different characteristics due to component variability. The full utility of the simulator can only be achieved with a good design and careful characterization of each unit.

Since this pulse measurement method has not been optimized, and all types of samples have not been tested under various combinations of temperature, magnetic field and sample orientation, these results are considered preliminary. It may be possible to reduce voltage noise and the effect of ground loops in this measurement method. Much more experimental investigation is needed to address completely possible differences in I_c determined by different methods.

The pressure contacts have not yet been optimized. Changes in design, pressure and materials may reduce the contact resistance and improve the conduction of heat to the liquid nitrogen bath. The degradation from soldering contacts in this case was more than the observed effect of heating with zero applied field. Additionally, more narrow patterned films would significantly lower power dissipation. The 500 μm wide film was selected to study the effect at the higher currents.

A similar comparison of two measurement methods has been performed using this passive simulator[11]. This reference compares a lock-in technique (d.c. and a.c. transport current method) to the d.c. method. The comparison showed good agreement between the lock-in and d.c. methods, which is consistent with the comparison presented here. It was also observed that noise of the lock-in technique was significantly higher than that of the d.c. method.

Conclusions

The passive simulator is well suited for a simple comparison of different measurement methods and for interlaboratory comparisons of measurements. Results of comparisons using a passive simulator may not be sufficient because the simulator cannot emulate all of the subtle effects of a superconductor. However, the passive simulator is an important first step in determining the major sources of critical current measurement variability. On the passive simulator, the d.c. and pulse methods gave the same critical current to within 0.2%.

The initial comparison of d.c. and pulse methods to determine the critical current of superconductive samples indicated that the two methods can give the same result, within 1%, for samples with low contact heating and low heat flux. Small differences, less than 4%, were observed for a thin film specimen measured with 26 mW (≈ 3 W cm^{-2}) of contact heating. When heating was a factor, the time constant of the transition from pulse to d.c. behaviour was of the order of 0.7 s. Pulse current measurements in an applied magnetic field are more difficult because the motion caused by the pulsed Lorentz force interferes with the measurement.

Acknowledgements

The author extends his thanks to R.H. Ono (Cryoelectronic Metrology Group) for thin film samples, J. Moreland for bulk samples, A.N. Srivastava for assisting the preparation of this paper, and T.C. Stauffer and R.M. Folsom for assisting with the measurements and instrumentation. The passive circuit is based on an idea by J.W. Ekin and J. Brauch of NIST.

References

1 **Goodrich, L.F. and Fickett, F.R.** Critical current measurements: a compendium of experimental results *Cryogenics* (1982) **22** 225–241
2 **Goodrich, L.F. and Bray, S.L.** High T_c superconductors and the critical current measurement *Cryogenics* (1990) **30** 667–677
3 **Bray, S.L. and Goodrich, L.F.** Current supply for high T_c superconductor testing *Meas Sci Technol* (1990) **1** 491–494
4 **Kwak, J.F., Venturini, E.L., Baughman, R.J., Morosin, B. and Ginely, D.S.** High critical currents in polycrystalline Tl–Ca–Ba–Cu–O films *Cryogenics* (1989) **29**(*3A*) 291
5 **Salama, K., Selvamanickam, V., Gao, L. and Sun, K.** High current density in bulk $YBa_2Cu_3O_x$ superconductor *Appl Phys Lett* (1989) **54** 2352
6 **Ekin, J.W., Larson, T.M., Bergren, N.F., Nelson, A.J., Swartzlander, A.B., Kazmerski, L.L., Panson, A.J. and Blankenship, B.A.** High T_c superconductor/noble-metal contacts with surface resistivities in the 10^{-10} Ω cm^2 range *Appl Phys Lett* (1988) **52** 1819
7 **Goodrich, L.F. and Bray, S.L.** Current ripple effect on superconductive d.c. critical measurements *Cryogenics* (1988) **28** 737–743
8 **Goodrich, L.F. and Bray, S.L.** Integrity tests for high-T_c and conventional critical-current measurement systems *Adv Cryog Eng Mat* (1990) **36A** 43–50
9 **Kimura, Y., Higuchi, N., Meguro, S., Takahashi, K., Uyeda, K., Ishihara, T., Inukai, E. and Umeda, M.** Round robin tests of T_c and I_c on $YBa_2Cu_3O_x$ *IEEE Trans Magn* (1989) **MAG-25** 2033
10 **Soulen, R.J., Jr** Personal communication, Naval Research Laboratory, Washington DC, USA (1989)
11 **Moreland, J., Li, Y.K., Goodrich, L.F., Roshko, A. and Ono, R.H.** Novel procedure for mapping the $J_c-H_{c2}-T_c$ surface and its application to high temperature superconductors *Science and Technology of Thin-Film Superconductors 2* (Proceedings of the Second Conference on the Science and Technology of Thin-Film Superconductors, Denver, Colorado, USA, April/May 1990) Plenum Publishing Corporation, New York, USA (1990) 429–438